Check for updates

Vortex fluidic device-driven production of medium-chain free fatty acids for organic cosmetic ingredients

Xuejiao Cao,[a] Caterina Selva, [iD] †[b] Jonathan A. Campbell,[a] Vincent Bulone, [iD] [b] Xuan Luo, [iD] [a] M. Ajanth Praveen,[b] Youhong Tang [iD] [a] and Colin L. Raston [iD] *[a]

Medium-chain free fatty acids (MCFFA), such as capric acid and caprylic acid, are valuable ingredients in organic cosmetics and are well-known for their antibacterial properties. To produce such MCFFA, conventional triglyceride saponification methods are commonly employed; however, these methods are often inefficient, energy-intensive, and fail to meet sustainable MCFFA production standards. This study utilises a Vortex Fluidic Device (VFD), a thin-film processing technology, to enhance the production efficiency and the yield of MCFFA from Palmester oil, composed of 40% capric acid (C10) and 60% caprylic acid (C8). Operating at 5000 rpm in continuous flow mode at 70 °C, the VFD achieved a 95% yield of MCFFA with 96% purity, representing a 1.44-fold increase in yield compared to the conventional water-bathing method under the same processing conditions. In contrast, the benchtop methods yielded 37% fatty acid ethyl esters as byproducts with significantly lower purity. Rheological analysis revealed that the MCFFA produced *via* VFD, resulting from the ethanol used in the saponification process, exhibited low viscosity. DSC analysis confirmed the thermal stability of the product, underscoring its potential in industrial applications. Moreover, MCFFA showed superior antibacterial activity, producing larger inhibition zones compared to commercial capric acid and caprylic acid at the same concentrations. These findings highlight the potential of VFD as a novel technology for producing high-purity MCFFA with enhanced antibacterial efficacy, supporting its application in organic cosmetic formulations.

Sustainability spotlight

This study presents a sustainable method for producing cosmetic-grade medium-chain free fatty acids (MCFFA) from Palmester oil using vortex fluidic device (VFD) technology. The process significantly enhances yield and purity while reducing reaction time and energy consumption, demonstrating strong alignment with green chemistry principles. By utilising a renewable feedstock and replacing the energy-intensive processing method, the approach supports UN Sustainable Development Goals 12 (Responsible Consumption and Production) and 3 (Good Health and Well-Being). The resulting MCFFA exhibits superior antibacterial efficacy and favourable formulation properties, offering a high-performance, bio-based alternative for eco-conscious applications in organic cosmetic products.

1 Introduction

The demand for organic cosmetics has surged in recent years as consumers become increasingly conscious of the ingredients in skincare products and their environmental impact.[1] Organic cosmetics are valued for their purity, safety, and contribution to sustainability,[2] aligning with the United Nations' Sustainable Development Goals (SDGs), such as responsible consumption and production (SDG 12) and good health and well-being (SDG 3). Various regulatory bodies have established standards to ensure these products meet stringent criteria. In the United States, the U.S. Department of Agriculture (USDA) Organic Certification mandates that products labelled as organic must contain at least 95% organically produced ingredients. In Europe, the Cosmetic Organic and Natural Standard (COSMOS) requires all products to have at least 95% plant-based ingredients, 20% of the total ingredients to have "organic" certification, and 50% to have "natural" certification.[3] Similarly, Ecocert, one of the oldest certification bodies, stipulates that at least 95% of the total ingredients must be natural or of natural origin, with a minimum of 10% of the total ingredients by

[a]*Flinders Institute for Nanoscale Science and Technology, College of Science and Engineering, Flinders University, Bedford Park, SA 5042, Australia. E-mail: colin. raston@flinders.edu.au*

[b]*College of Medicine and Public Health, Flinders University, Bedford Park, SA 5042, Australia*

† Present address: School of Agriculture, Food and Wine, Waite Research Institute, University of Adelaide, Waite Campus, Urrbrae, SA 5064, Australia.

weight coming from organic farming. These standards ensure that organic cosmetics are free from parabens, genetically modified organisms, and artificial fragrances, guaranteeing product safety and environmental sustainability.[4] In organic cosmetics, plant-based ingredients are sourced and minimally processed without synthetic chemicals or irradiation, preserving their natural structure while ensuring the integrity and purity of the final product.[5] COSMOS-approved processes include physical methods like grinding and extraction, as well as biological processes such as fermentation. Chemical methods like hydrolysis, esterification, and saponification are also allowed if they are eco-friendly and do not produce synthetic molecules.[6] The production processes for organic ingredients aim to reduce environmental impact through sustainable sourcing, energy-efficient manufacturing, and eco-friendly packaging.[4,6]

Plant-based caprylic acid (C_8) and capric acid (C_{10}) are medium-chain free-fatty acids (MCFFA) that are highly valued in the cosmetic industry.[7] In skincare formulation, MCFFA penetrates skin easily which ensures deep hydration and long-lasting effects. MCFFA also enhances the product efficacy by acting as a stabilising solvent for other active ingredients. Additionally, MCFFA improves the skin barrier, preventing moisture loss and protecting against environmental stressors.[8,9] In the fragrance industry, they are used as carriers and solvents, ensuring consistent scent profiles and enhanced longevity. Furthermore, MCFFA has been explored as an active ingredient in outdoor cosmetics, serving as a natural insect repellent that protects against insect bites while promoting skin health, offering a safer alternative to chemical-based repellents.[10,11] In cleaning products, the antimicrobial properties of MCFFA make them ideal for disinfecting surfaces and eliminating harmful bacteria and fungi.[12,13] Especially, caprylic acid and capric acid have been reported for their antibacterial and antifungal activities, being effective ingredients against a broad range of microorganisms, including *Candida albicans*, *Staphylococcus aureus*, and *Escherichia coli*.[14] As microbial contamination is a significant concern in the cosmetic industry, MCFFA can act
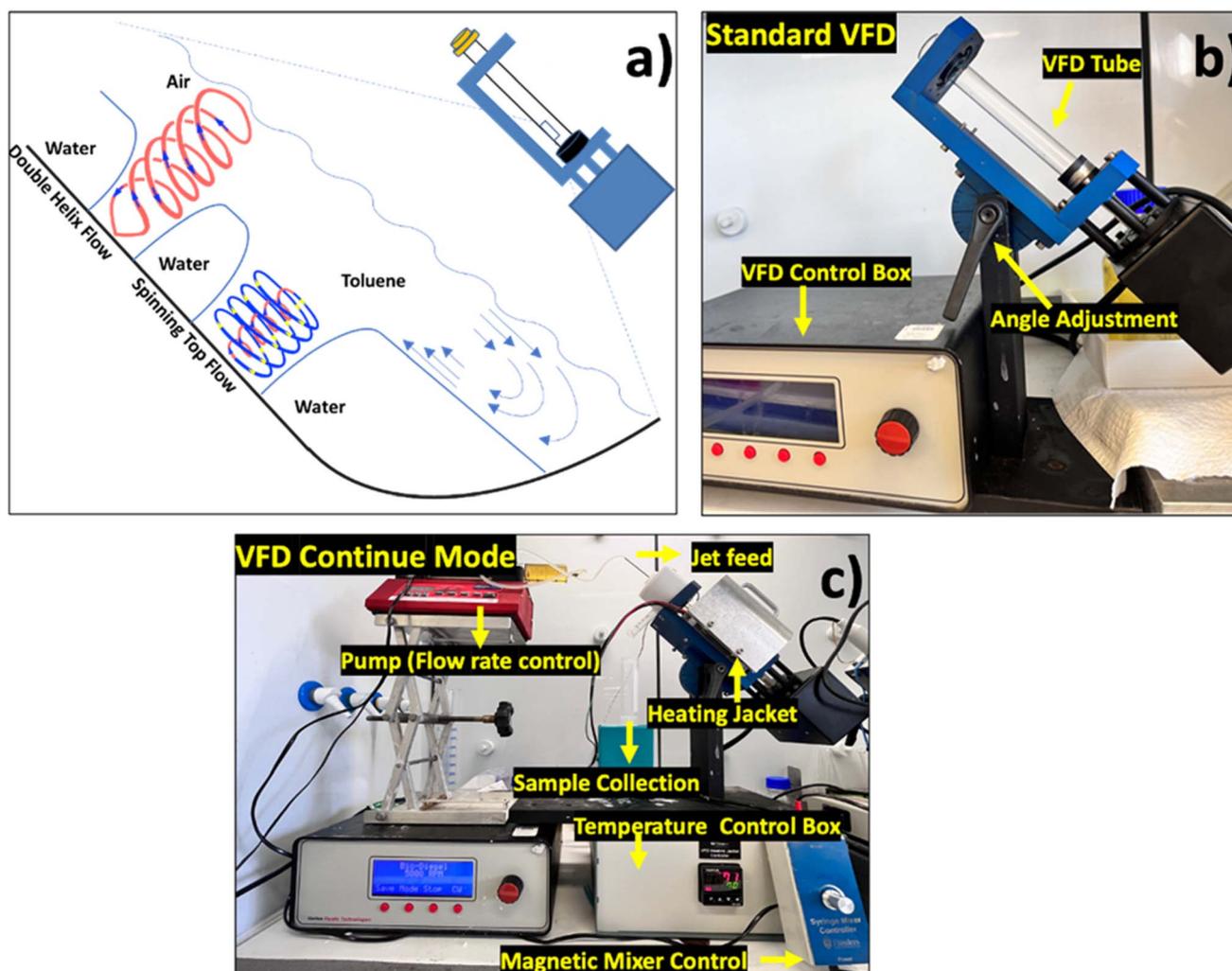

Fig. 1 Schematics of the Vortex Fluidic Device (VFD). (a) The two topological flows, both with micron/submicron dimensions, are generated in the thin film of liquid during processing. (b) A photo of VFD in confined mode processing, (c) a photo of VFD in continuous flow mode of processing.

as a natural antibacterial agent for the organic cosmetic industry, offering versatile functions for organic cosmetic formulations while complying with stringent organic cosmetic standards.

Traditional MCFFA production relies on triglyceride saponification, which is energy-intensive and inefficient when using conventional benchtop methods. This inherent inefficiency underscores the necessity of developing new technologies that prioritise sustainability and energy efficiency. The Vortex Fluidic Device (VFD), as an efficient and one-step and energy-efficient processing platform, meets the sustainable processing requirements. As shown in Fig. 1a, the VFD utilises thin film technology that enhances chemical reactions through high-shear stress. It consists of a rapidly rotating and inclined quartz tube that creates a thin liquid film against the tube's inner surface. The liquid thin film is subjected to intense shear forces, which drive the chemical reactions. Within the VFD, two distinct types of topological flows prevail, both down from micron to submicron dimensions. The spinning top (typhoon-like) flow from the Coriolis force from the hemispherical base of the tube and the double helical flow influenced by Faraday wave eddies.[15,16] These fluid flows act as driving forces to initiate reactions, significantly increasing processing efficiency. Recent studies have further clarified the fundamental mechanisms underlying VFD processing. Alotaibi[17,18] demonstrated that UV irradiation of aqueous thin films within the VFD induces photo-contact electrification under the high shear, generating reactive oxygen species (H_2O_2, $\cdot OH$, $O_2^{\cdot-}$) which reduce metal ions without the need for added reducing reagents, as a reagent-free, green-chemistry process. Complementarily, another study[19] revealed that magnetic-field-modulated shear flow in the VFD produces chiral lemniscate patterns through Lorentz-force-driven spin alignment, confirming that magnetic fields can influence materials orientation and reactivity. The VFD has proven its capability across various applications in broad areas, including chemistry,[20] biology,[21] food processing,[22] and medical science.[23] These applications include self-assembly of C_{60},[24] processing of liposomes,[20] formation of nanogold,[25] fabrication of 2D materials[26] and hydrogels,[21] biomarker diagnostics,[23] and enhancing shampoo function.[27] This versatility highlights its potential to revolutionise material processing, in line with the processing standards in organic cosmetics.

The VFD operates in different modes tailored to specific applications. The confined mode operation, shown in Fig. 1b, targets small-scale reactions, where 1–2 mL of liquid is added to a quartz tube. The heating jacket positioned around the rotating tube offers external heat to further drive a reaction. The continuous flow mode (Fig. 1c) allows for the constant feeding and processing of reagents by using an external pump to introduce them through a jet feed at a controlled flow rate. This mode of operation can be used for efficiently processing large volumes and therefore allows scalability of the process. It has been used in biofuel production,[28] large-scale chemical synthesis,[29] pharmaceutical manufacturing,[30] and organic dye degradation,[31] offering scalability from laboratory research to more practical industry applications.

COSMOS-approved Palmester oil, composed of 40% capric acid and 60% caprylic acid, is a widely recognised emollient and moisturiser in organic cosmetics.[32] In this study, it is utilised as an organic feedstock for the sustainable production of MCFFA through a VFD-enhanced saponification process. While saponification is a widely used process, this study employs VFD processing instead of conventional benchtop methods to enhance reaction efficiency, reduce energy consumption, and improve product purity. The confined mode of VFD operation is used for optimising the parameters, while the continuous flow mode is pursued for scaling up. Traditional water bathing served as a control to compare the saponification efficiency. The antibacterial efficacy of the MCFFA produced by the VFD was assessed against that of commercially available single MCFFA to evaluate its potential use in cosmetic formulations for enhancing antimicrobial properties. By leveraging the capabilities of the VFD, this study demonstrates a more efficient and eco-friendly approach for producing high-purity MCFFA from Palmester oil, thereby promoting sustainable practices in the development of organic cosmetic ingredients.

2 Materials and methods

2.1 Materials

Palmester oil and ethanol were provided by Plantworx Pty Ltd (Adelaide, Australia). Analytical grade solvents, including chloroform, chloroform-*d*, NaOH, capric acid, caprylic acid, and 2,2-diphenyl-1-picrylhydrazyl (DPPH) were purchased from Sigma-Aldrich.

2.2 MCFFA production

The MCFFA was derived from Palmester oil through a saponification reaction by mixing the oil with a 20% NaOH-ethanol solution at a ratio of 1 : 2. The rotational speeds and processing time were optimised using the confined mode of VFD, followed by scale-up production using its continuous flow mode. The results were compared to the water-bathing method, and the production yield was calculated using eqn (1).

$$\text{MCFFA yield} = \text{mass of MCFFA/mass of raw Palmester oil}$$

(1)

2.2.1 MCFFA optimised production in VFD confined mode. The VFD was equipped with a quartz tube of 20 mm external diameter and positioned at a tilt angle (θ) of 45° relative to the horizontal axis. To compare saponification efficiency in VFD, the rotation speeds of 5000 and 7750 rpm were tested over 1 h. Subsequently, the processing time was reduced to 40, 20, and 10 min for further evaluation. While the rotational speed and processing time were varied to determine the optimal operating conditions, the heating jacket was maintained at 70 °C throughout all VFD experiments as a fixed operational parameter to ensure consistency and comparability. A NaOH solution was prepared by dissolving 20 g of solid in 50 mL water, followed by mixing it with 50 mL ethanol. Then, 0.6 mL of oil and 1.2 mL NaOH-ethanol solution were added to the quartz tube.

After reacting in the tube for the designated time, the mixture was allowed to cool to room temperature. The samples were subsequently washed with distilled water, and the pH was adjusted to 1 using HCl. Finally, the samples were collected after centrifugation at $9000g$ for 20 min.

2.2.2 MCFFA scale-up production in VFD continuous flow mode. The continuous flow mode VFD was used to scale up MCFFA production. A mixture of 30 mL of the oil and NaOH-ethanol was prepared and loaded into a 50-mL glass syringe. The flow rate was set to 0.5 mL min^{-1} (1 h processing time in total), and the VFD rotational speed was derived from the optimisation experiments as described in Section 2.2.1. Magnetic mixer control was employed to gently mix the oil and NaOH-ethanol mixture, preventing phase separation of the starting solution before loading to the syringe pump.

2.2.3 MCFFA production in bench-top method. The bench-top operation was conducted in a water bath with a magnetic stirrer (MSH-300, Biosan) to maintain temperatures of 70 °C or 100 °C for comparative analysis, while all other conditions remained consistent with those used in VFD processing. A 30 mL mixture was processed in the water bath for 1 h at each temperature to evaluate the effect of thermal conditions on MCFFA production.

2.3 MCFFA characterisation

2.3.1 Nuclear magnetic resonance. Proton nuclear magnetic resonance (^{1}H NMR, Bruker 600 MHz Avance III Spectrometer) spectra of samples were acquired using a 600 MHz Bruker spectrometer. Standard quantitative parameters, including a delayed pulse (D1) of 10.00 and 32 scans, were employed for oil and MCFFA assessment. 10 μL of each sample was diluted with 0.5 mL D-chloroform in NMR tubes prior to recording the spectra.

2.3.2 Fourier transform infrared spectroscopy. Fourier transform infrared spectroscopy (FTIR, Nicolet Nexus 870) was carried out to determine functional groups present in Palmester oil and MCFFA. Attenuated total reflectance (ATR) in conjunction with infrared spectrometry using a Fourier transform was employed for sample testing. Here, 0.1 mL of each sample was placed on the diamond crystal of the ATR FTIR spectrometer and scanned over 500–4000 cm^{-1} with 8 scans, and a resolution of 4 cm^{-1}.

2.3.3 Gas chromatography-mass spectrometry. The samples were tested by gas chromatography-mass spectrometry (GC-MS),[33] which was conducted using a Varian CP-3800 gas chromatography unit coupled with a 2200 Saturn MS detector. The injection temperature was set at 40 °C, with a gradual increase to 300 °C. A reverse-phase column (30 m × 25 mm × 0.25 mm) was used, and NIST 05 molecular recognition software was employed for data analysis. 10 μL of sample was diluted with 1 mL of chloroform in a glass vial for the analysis.

2.3.4 Viscosity and rheology. The sample rheological properties were determined using a Brookfield Rheometer (TA Instruments RA2000) equipped with a thermo-container and a programmable temperature controller. The thermo-container includes a sample chamber and spindle. The temperature was maintained at 25 °C, with a 10 mm gap setting, and 1.5 mL of each sample was placed on the plate for all measurements. For the strain sweep, the shear frequency was controlled at 6.283 rad s^{-1}, with strain values ranging from 1% to 10 000%. The viscosity profile was tested in flow mode with the spindle set to a shear rate from 0.01 to 500.00 rad s^{-1} at 5 s intervals.

2.3.5 Differential scanning calorimeter. The thermal stability of samples was determined using TA Instruments DSC-2930 and DSC-8000 Differential Scanning Calorimeters. The equipments were calibrated with pure indium, and the empty aluminium pan was used as a reference. The thermal stability of samples was tested by the DSC-2930, utilising T-zero sealed pans. Nitrogen gas flowed at a rate of 50 mL min^{-1}, and the temperature range was set from −70 °C to 300 °C, with a heating rate of 10 °C min^{-1}. For the thermal oxidation test, around 0.2–0.5 mg of each sample was weighed into open aluminium pans and placed in the DSC-8000 sample chamber. The gas flow rate was set at 20 mL min^{-1} for both nitrogen and air. The temperature range was 25 °C to 300 °C, with a heating rate of 10 °C min^{-1}. The onset point was determined as the intersection of the extrapolated baseline and the horizontal line of the isotherm, marking the onset of oxidation.

2.4 Bioactivities of MCFFA

2.4.1 Antibacterial efficiency. *Staphylococcus aureus* subsp. *aureus* ATCC 25923 (Gram-positive) and *Escherichia coli* strain B ATCC 11303 (Gram-negative) were used to evaluate antibacterial activity. For each species, individual bacterial colonies were picked and transferred to 10 mL Luria–Bertani (LB) broth (Merck, Germany) and grown overnight at 37 °C with shaking at 250 rpm. The bacterial inoculum was adjusted to an OD$_{600}$ of 0.1, corresponding to $\approx 1 \times 10^7$ CFU mL^{-1} for *S. aureus* and $\approx 1 \times 10^8$ CFU mL^{-1} for *E. coli* by diluting with fresh LB medium. The surface of LB agar plates was inoculated with 200 μL of bacterial suspension, which was spread evenly to create a uniform bacterial lawn. A sterile cork borer was used to create 7 mm diameter wells, and 30 μL of each sample at the desired concentration was added to the wells. Plates were incubated overnight at 37 °C. To assess antibacterial activity, the diameter of the zones of inhibition (ZOI) was measured using a ruler, with larger diameters indicating greater antibacterial efficacy. A 50% ethanol solution was used as the negative control, and ampicillin (50 μg mL^{-1}) was used as the positive control. The MCFFA was initially prepared as 250 g per L stock solution in 50% ethanol solution and subsequently serially diluted in MilliQ water to concentrations of 100, 50, 25, and 12.5 g L^{-1}. Commercial capric acid and caprylic acid were tested under the same conditions to evaluate the potential synergistic effect of the MCFFA on antibacterial efficiency.

2.4.2 DPPH radical scavenging activity. A 0.1 mM solution of DPPH in ethanol was freshly prepared to assess the antioxidant activity of the samples. For each assay, 180 μL of the DPPH solution was pipetted into a 96-well microplate, followed by the addition of 20 μL of the sample to be tested. The reaction mixtures were incubated at 25 °C for 30 min in the dark to prevent photodegradation of the DPPH. After incubation, the

absorbance was measured at 517 nm using a microplate reader (SPECTROstar Nano, BMG LABTECH). The DPPH inhibition was calculated as a percentage with respect to the blank solution.

3 Results and discussion

3.1 Optimisation of MCFFA production using VFD (confined mode)

The efficiency of capric acid and caprylic acid production is highly dependent on the saponification process, wherein the triglyceride structure of Palmester oil is broken down in the presence of a catalyst and heat.[34] During this process, three fatty acid molecules are cleaved from the glycerol backbone, which can be distinguished by characteristic peaks in ^{1}H NMR spectra.

The triglyceride structure of Palmester oil is marked by the symmetric hydrogen atoms in the glycerol backbone,[35] contributing to peaks a and c at 4.34 and 4.19 ppm in Fig. 2a. Additionally, the hydrogen atoms attached to the middle carbon (peak b) of the glycerol are observed at 5.3 ppm. The absence of these three peaks indicates the completion of the saponification process, while the presence of any of these peaks suggests the presence of mono-, di-, or triglycerides, where not all fatty acids have been cleaved from glycerol.[36]

The rotational speed in the VFD affects the thickness of the liquid film and the fluidic flows applied during processing, resulting in different reaction outcomes. The peak a′ at 4.17 ppm in Fig. 2b is observed for the compounds produced in VFD confined mode at 7750 rpm for 1 h, corresponding to the methylene protons (–CH$_2$–) of the ethyl group in fatty acid ethyl
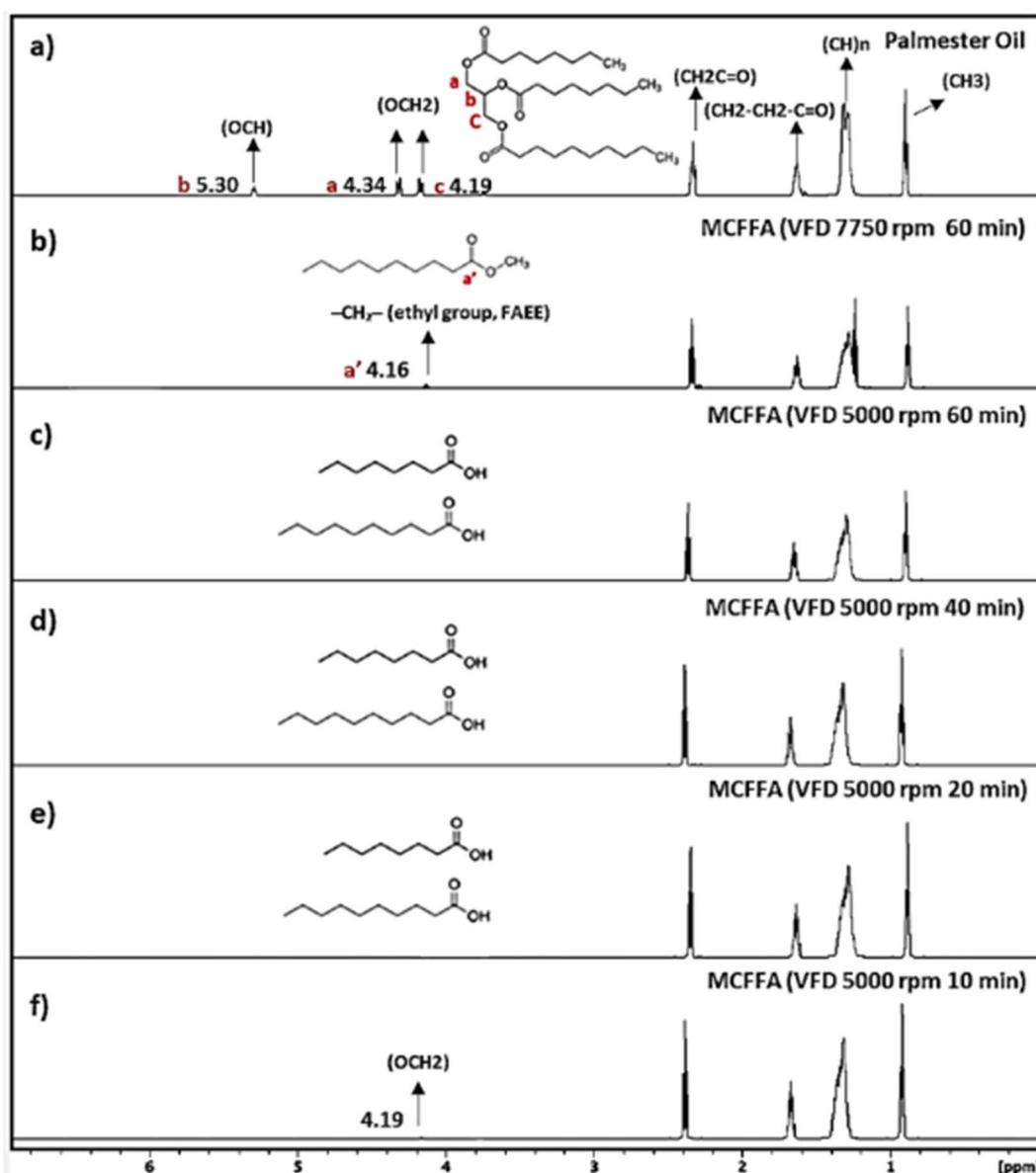

Fig. 2 ^{1}H NMR spectra of MCFFA processed in VFD confined mode. The VFD was operated at 5000 rpm and 7750 rpm for 1 h each at 70 °C, with the processing times then reduced to 40, 20, and 10 min. (a) ^{1}H NMR spectra of Palmester oil. (b) ^{1}H NMR spectra of MCFFA produced using the VFD at 7750 rpm for 60 min. (c–f) ^{1}H NMR spectra of MCFFA produced using the VFD at 5000 rpm for 60, 40, 20, and 10 min, respectively.

ester (FAEE) structure,[37,38] which is the byproduct of the MCFFA production process. The formation of FAEE originates from the ethanol present in the NaOH-ethanol saponification solution described in Section 2.2 for MCFFA production, where liberated fatty acids can undergo secondary esterification with ethanol, particularly under prolonged reaction times or elevated temperatures. As shown in Fig. 2c, no peaks are present between 4.2 and 5.3 ppm for the product processed using VFD in the confined mode at 5000 rpm after 1 h, indicating complete saponification. Higher rotational speeds create thinner films and greater shear forces, enhancing mass and heat transfer, which accelerates reaction rates but also promotes secondary reactions, such as ethyl ester formation. This aligns with previous studies showing increased fatty acid methyl ester yields at higher speeds.[33] In this study, 5000 rpm was optimal for MCFFA production, balancing efficient mixing and reaction control while minimising byproduct formation.

Across various processing times—1 h, 40 min, 20 min, and 10 min—in the VFD confined mode at 5000 rpm, a 20-min processing time was found optimal for achieving high-purity MCFFA products. The ^{1}H NMR spectra from the 10-min process exhibited residual signals between 4.2 and 5.3 ppm (Fig. 2f), showing residual unreacted glycerides. The VFD confined mode is an ideal choice for small-scale trial experiments as it allows precise control over reaction time, temperature, and rotational speed, thereby enhancing mixing efficiency while minimising resource and energy consumption.[39] This approach is particularly advantageous for optimising reaction conditions before scale-up, as it ensures efficient use of materials, reduces waste, and aligns with environmentally friendly and sustainable processing practices.

3.2 Scale-up of MCFFA production using VFD (continuous flow mode)

The VFD continuous flow mode was employed to scale up MCFFA production from Palmester oil, along with a traditional water bath for comparison. According to the ^{1}H NMR spectra (Fig. 3a), the products processed using VFD continuous mode showed no residual triglyceride peaks or the presence of FAEE.

In contrast, the products from water bath processing at both 70 °C and 100 °C exhibited an FAEE peak at 4.17 ppm, indicating the presence of C=O in FAEE. As the temperature increases, the intensity of the peak in the ^{1}H NMR spectra of products from the water bath processing decreases. Although higher temperatures enhance saponification efficiency using a water bath, they do not align with clean production and sustainable processing standards due to increased energy consumption.[40] The VFD processing at 70 °C achieved significantly higher purity of MCFFA with lower energy input, as shown in Table 1, demonstrating 18% of energy consumption of the control trial using a magnetic stirrer. The energy consumption was calculated based on the maximum input, with specific speed-dependent values to be explored in future studies. In this work, the standard VFD operated under the continuous-flow mode proved effective for delivering clean, high-purity MCFFA under mild conditions while maintaining stable product throughput, demonstrating its potential for semi-industrial applications. Although this study employed the standard VFD, our group has successfully utilised an upsized 50 mm-OD VFD for large-scale cosmetic FAEE synthesis,[41] and its continuous-flow capabilities are being developed. This ongoing engineering effort aims to reproduce the analogous thin-film hydrodynamics and high-shear efficiency with higher throughputs relative to the 20 mm OD diameter VFD, a route to establishing a realistic and scalable technological pathway toward the sustainable, industrial-scale production of MCFFA and other bio-based cosmetic ingredients.

The purity of MCFFA products from the scale-up production was further verified using FTIR spectra. As shown in Fig. 4a, there is no wide absorbance band between 3500 cm^{-1}

Table 1 Energy consumption comparison of VFD and magnetic string device

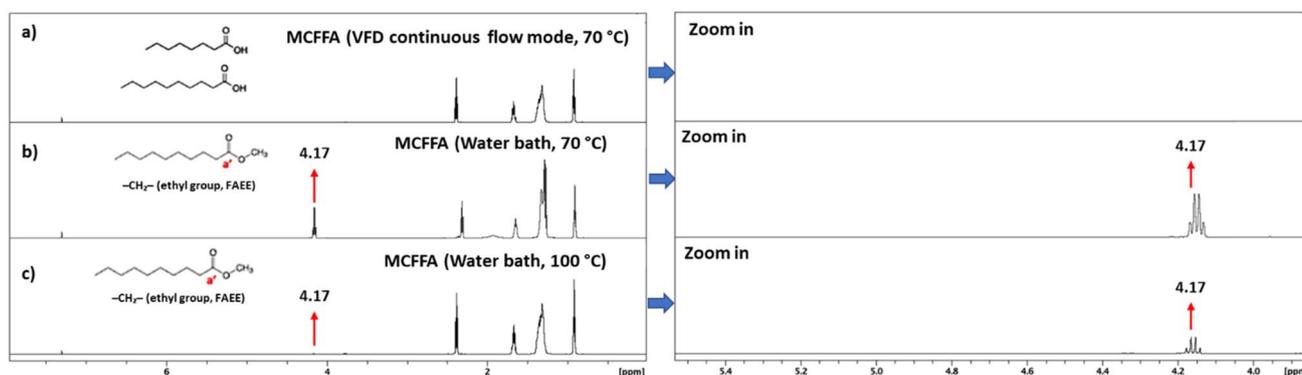| Device	Power (W)	Energy input (kWh)
Magnetic stirrer (MSH-300, Biosan)	825	0.825
VFD (5000 rpm with heating jacket)	145	0.145

Fig. 3 The ^{1}H NMR spectra of MCFFA were produced using the VFD continuous flow mode and a water bath. The VFD was operated at the rotational speed of 5000 rpm at 70 °C, with a flow rate of 0.5 mL min^{-1}. The water bath was set to 70 °C and 100 °C. A total volume of 30 mL was processed over 1 h for all methods. (a) ^{1}H NMR spectra of MCFFA produced using the VFD in continuous-flow mode at 70 °C. (b and c) ^{1}H NMR spectra of MCFFA produced using the water bath method at 70 °C and 100 °C, respectively.
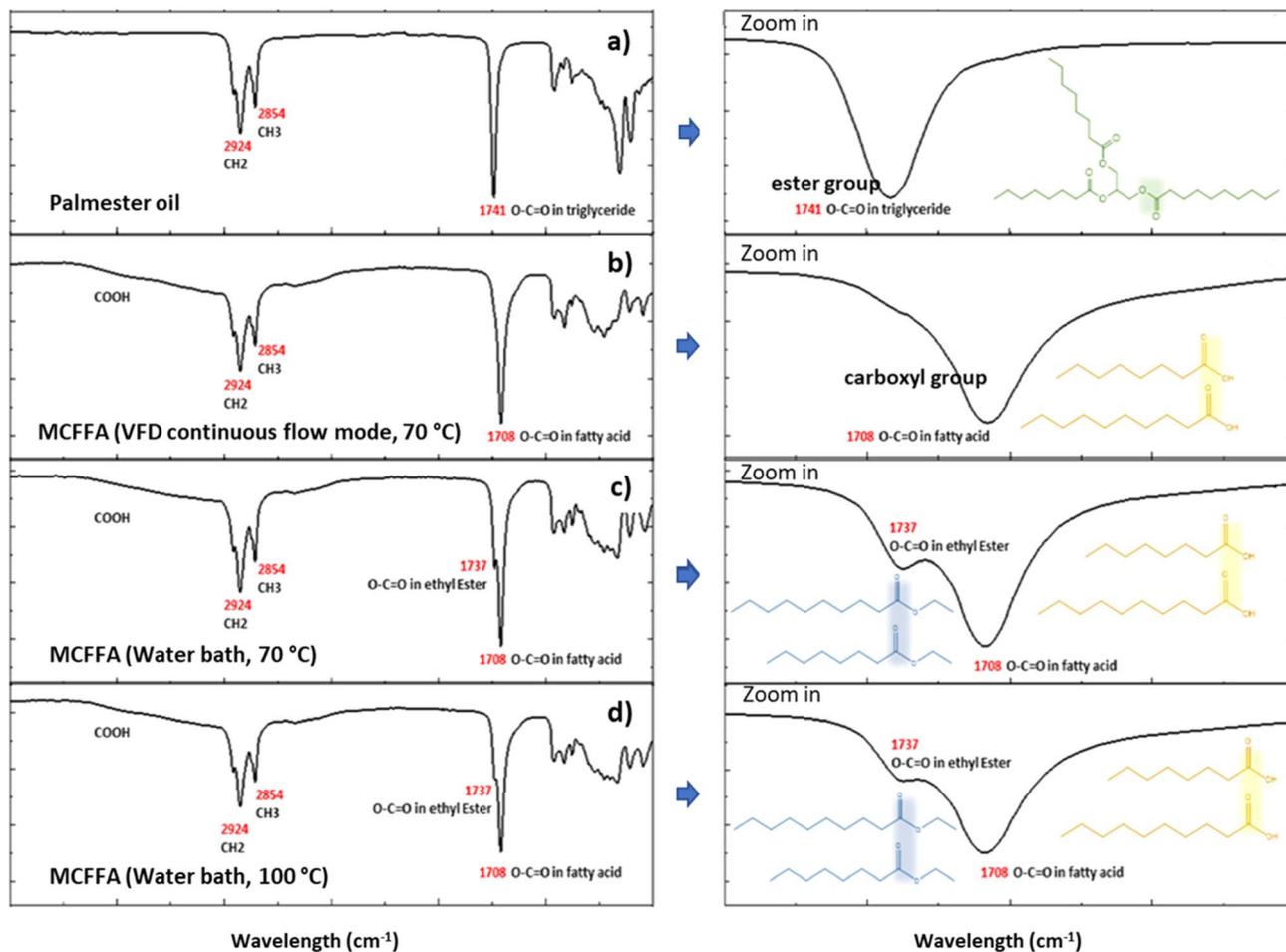
Fig. 4 The FTIR spectra of MCFFA were processed in VFD continuous flow mode and a water bath. The VFD was operated at a rotational speed of 5000 rpm in continuous mode at 70 °C, with a flow rate of 0.5 mL min^{-1}. The water bath was set to 70 °C and 100 °C. A total volume of 30 mL was processed over 1 h for all methods. (a) FTIR spectra of Palmester oil. (b) FTIR spectra of MCFFA produced using the VFD in continuous-flow mode at 70 °C. (c and d) FTIR spectra of MCFFA produced using the water bath method at 70 °C and 100 °C, respectively.

and 2900 cm^{-1} in Palmester oil. The CH$_2$ and CH$_3$ vibrations of the carbon chain are present at 2954 cm^{-1} and 2854 cm^{-1}, respectively, consistent with the recognised triglyceride structures in previous studies.[42] After saponification, a broad absorbance band between 3500 cm^{-1} and 2900 cm^{-1} appears in all FFA products, corresponding to the –COOH group, a characteristic absorbance band of FFA.[43] The C=O bond is present in the oil, MCFFA, and FAEE, and its position in the FTIR spectra reflects the purity of the FFA products.[44] The original oil shows a C=O absorbance band around 1741 cm^{-1} in Fig. 4a, while the C=O absorbance band for MCFFA is observed at 1708 cm^{-1} in Fig. 4b–d, confirming the formation of MCFFA. Notably, the products from the water bath treatment, shown in Fig. 4c and d, display a shoulder absorbance band at 1708 cm^{-1} with a lower-intensity absorbance band at 1737 cm^{-1}, indicative of the C=O group corresponding with FAEE. As the temperature of the water bath increases, the intensity of this FAEE C=O absorbance band decreases, consistent with the ^{1}H NMR results.

The composition and purity of MCFFA were confirmed by GC-MS (Fig. 5b). Four peaks are visible in the GC chromatogram shown in Fig. 5a, representing two main MCFFA products (capric acid/caprylic acid) and two FAEE byproducts (ethyl caprate/ethyl caprylate). Commercial capric acid and caprylic acid were used as references, as displayed in Fig. S1. Overall, the combined capric acid/ethyl caprate content accounted for 40% while caprylic acid/ethyl caprylate made up 60%. This is consistent with the fatty acid composition of Palmester oil. Notably, the four peaks exhibited variations in both percentage and intensity in the GC chromatogram under different processing conditions.

The MCFFA processed in a water bath at 70 °C showed a significantly higher percentage of FAEE (44%) than that processed in the VFD (5000 rpm) at 70 °C, which is 4%. Increasing the temperature to 100 °C in the water bath resulted in a higher MCFFA percentage (85%); however, the proportion of byproducts was still four times higher than that obtained using VFD. Moreover, the yield of MCFFA produced in the VFD was 95%, 1.44 times higher than the yield from the 70 °C water bath condition and 1.3 times higher than that from the 100 °C water bath experiment, as shown in Fig. 5c.
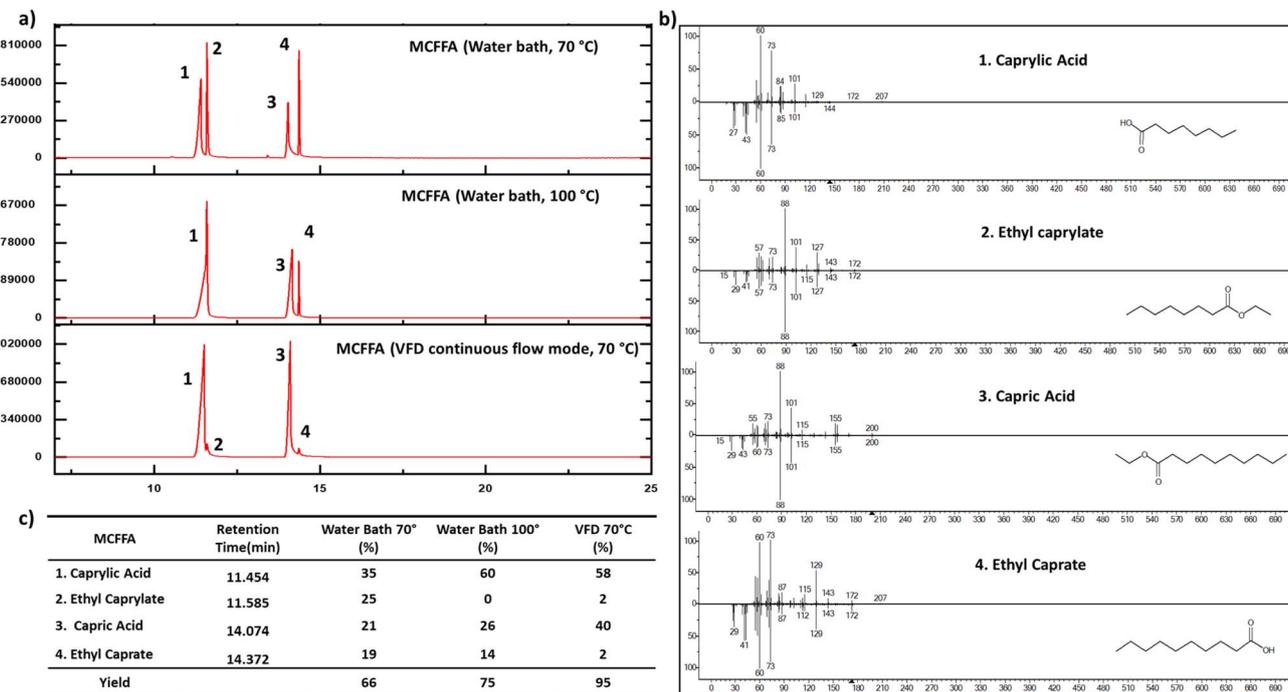
Fig. 5 The GC-MS spectra of MCFFA processed in VFD continuous mode and water bath conditions. The VFD was operated at 5000 rpm and 0.5 mL min^{-1} in continuous flow mode at 70 °C. The water bath was set to 70 °C and 100 °C. All methods processed 30 mL in 1 h. (a) GC spectra of MCFFA samples, showing the separation of components. (b) Mass spectra of four key peaks, identifying the molecular composition. (c) Percentage composition of each MCFFA component and the corresponding yield.

3.3 Rheology of MCFFA

Lipid ingredients with lighter textures present significant advantages in cosmetic formulations by reducing the greasy residue commonly associated with heavier oils.[45] It is reported that light oil has enhanced absorption and provides superior spreadability on the skin.[46] To assess these benefits, the rheological properties of the MCFFA were compared with those of Palmester oil. As shown in Fig. 6a and b, the MCFFA exhibits lower values of storage modulus (G') and loss modulus (G'') compared to Palmester oil, indicating that the MCFFA forms a less rigid, more fluidic structure, contributing to a lighter and less greasy sensory feel during application. The viscosity curves of both the oil and MCFFA demonstrate a shear-thinning behaviour at low shear rates in Fig. 6c, exhibiting characteristics of non-Newtonian fluids.[47] The viscosity test shows that MCFFA exhibits significantly lower viscosity than the original Palmester oil, which can be attributed to the simpler structure of MCFFA. In contrast, the triglycerides in Palmester oil have more extensive and complex chain–chain interactions, including physical entanglements, leading to higher viscosity.[47–50] At a shear rate of 0.01 s^{-1}, the viscosity of MCFFA is below 0.01 Pa s, indicating excellent fluidity. This low viscosity enhances spreadability, making MCFFA ideal for cosmetic formulations that provide a lightweight, non-greasy feel.[50]

3.4 Thermal stability of MCFFA

To examine their thermal behaviour, DSC analysis was conducted under both nitrogen and air atmospheres. These conditions simulate inert and oxidative environments, respectively, providing insights into their stability during industrial storage and processing. Although 300 °C exceeds the temperature range typically encountered in cosmetic applications, this upper limit was used to evaluate the onset of oxidative degradation or thermal polymerisation relevant to storage and processing. After each DSC run, the sealed pans were opened to visually examine the thermal residues.

Under nitrogen, Palmester oil exhibited a small exothermic peak around −33 °C (Fig. 7a), likely indicating partial melting followed by recrystallisation into a more stable polymorphic structure, possibly the β′ form, which is a metastable crystalline state of the oil.[51] Upon further heating, a sharp endothermic peak around 2 °C corresponded to the complete melting of crystalline material.[51] The MCFFA melted at 0.81 °C (Fig. 7b), significantly lower than that of pure capric acid and caprylic acid in Fig. S2a and c, which is consistent with eutectic behaviour and reduced molecular order.[52,53] As a result, the MCFFA produced in this study remain liquid and stable at ambient temperature, without crystallising or phase separating even after prolonged storage, which is highly advantageous for formulation handling, cold-chain-free storage, and consistent performance in cosmetic applications. After melting, Palmester oil exhibited no further thermal events up to 300 °C, indicating thermal stability under inert conditions. Its stability is further evidenced by the clear, oily residue remaining in the aluminium pan. In contrast, the heat flow of MCFFA dramatically decreased (endotherm) when the temperature reached 243 °C,
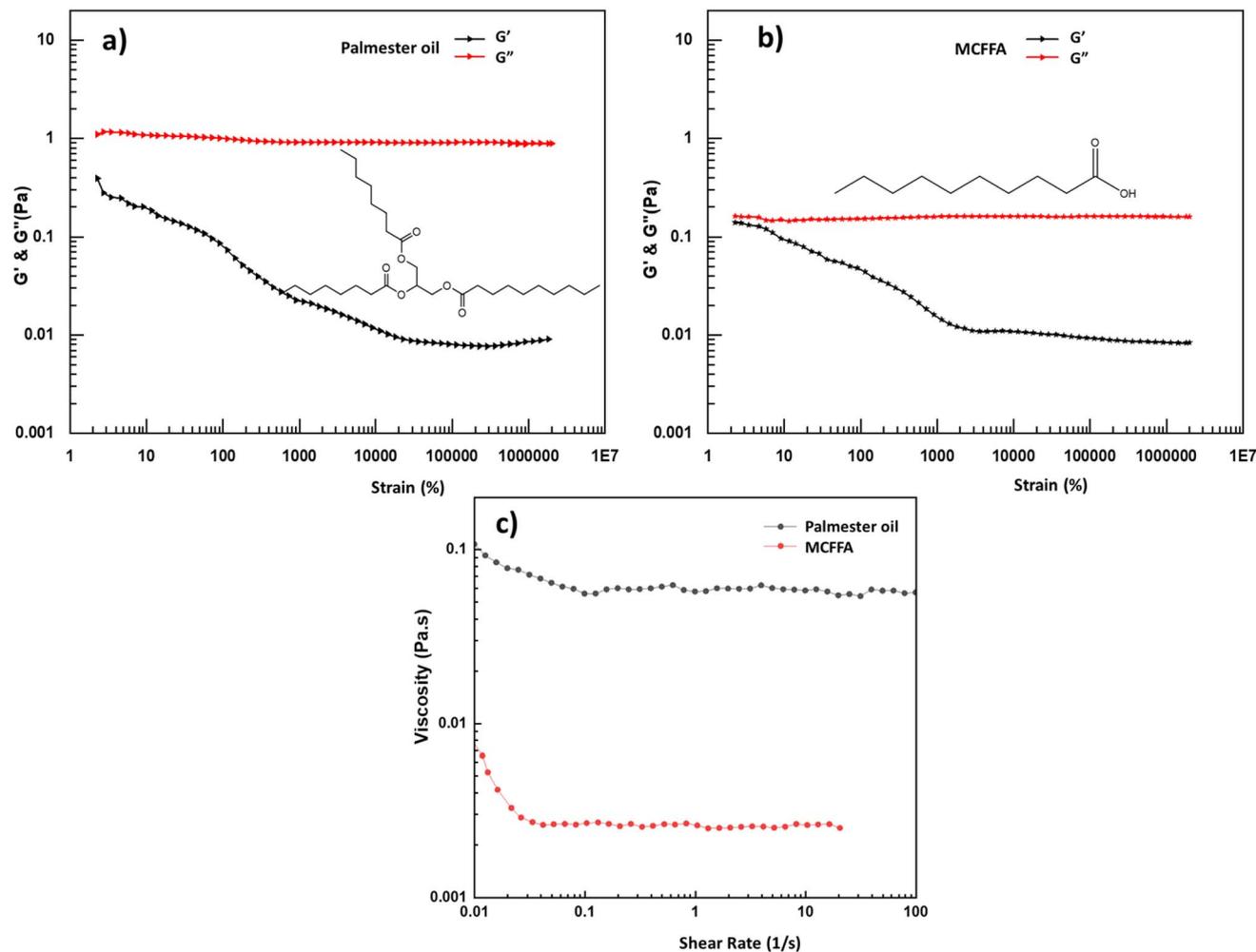
Fig. 6 Rheological properties of VFD-produced MCFFA and Palmester oil. The VFD was operated at 5000 rpm and 0.5 mL min^{-1} in continuous flow mode, at 70 °C. (a) Strain sweep of Palmester oil. (b) Strain sweep of MCFFA. (c) Viscosity of Palmester oil and MCFFA.

accompanied by the release of white vapour from the chamber. The residue-free pan suggests evaporation, which is consistent with the reported boiling points of caprylic and capric acids (230–260 °C). As pyrolysis generally leaves behind carbonaceous residues, with no such residue observed in the present study, the event is attributed to volatilisation rather than thermal decomposition.[54] Future studies using sealed-pan DSC with cyclic heating and cooling (−50 °C to 100 °C) could better represent practical cosmetic conditions.[54]

To assess the oxidative thermal stability of MCFFA, DSC was performed under air, exposing the samples to both heat and oxygen. Both Palmester oil and MCFFA remained stable below 150 °C, indicating suitability for cosmetic processing. However, the samples displayed oxidative/decomposition behaviours beyond this point. Palmester oil exhibited a strong exothermic peak at 321 °C, suggesting oxidative degradation of triglycerides into smaller oxygenated molecules, such as aldehydes, ketones, and hydroperoxides. These may break down further into CO_2 and H_2O, while incomplete oxidation left a yellowish, sticky residue,[55] as shown in Fig. 7c. In contrast, MCFFA showed an endothermic event at 182 °C, without a significant exothermic

peak, resembling the behaviour of pure capric and caprylic acids (Fig. S2c and d). The saturated chains in FFA are more prone to decomposition or oxidation at lower temperatures than triglycerides.[56] The dark residue left in the pan suggests carbonisation, where the material is only partially oxidised, undergoing incomplete thermal decomposition and leaving behind carbon-rich products (char) after heating. In short, Plamester oil undergoes oxidative cleavage, leading to exothermic decomposition.[57]

3.5 Antibacterial efficiency of MCFFA

The antibacterial properties of MCFFA are particularly valuable in organic cosmetics compared to synthetic antibacterial agents, as they are derived from natural sources and are biodegradable in an eco-friendly manner.[58] Additionally, mixtures of MCFFA have been reported to exhibit synergistic effects, outperforming individual fatty acids.[59] MCFFA, composed of 60% caprylic acid and 40% capric acid, has potential for bacterial resistance. *Staphylococcus aureus* (*S. aureus*), a Gram-positive bacterium, and *Escherichia coli* (*E. coli*),
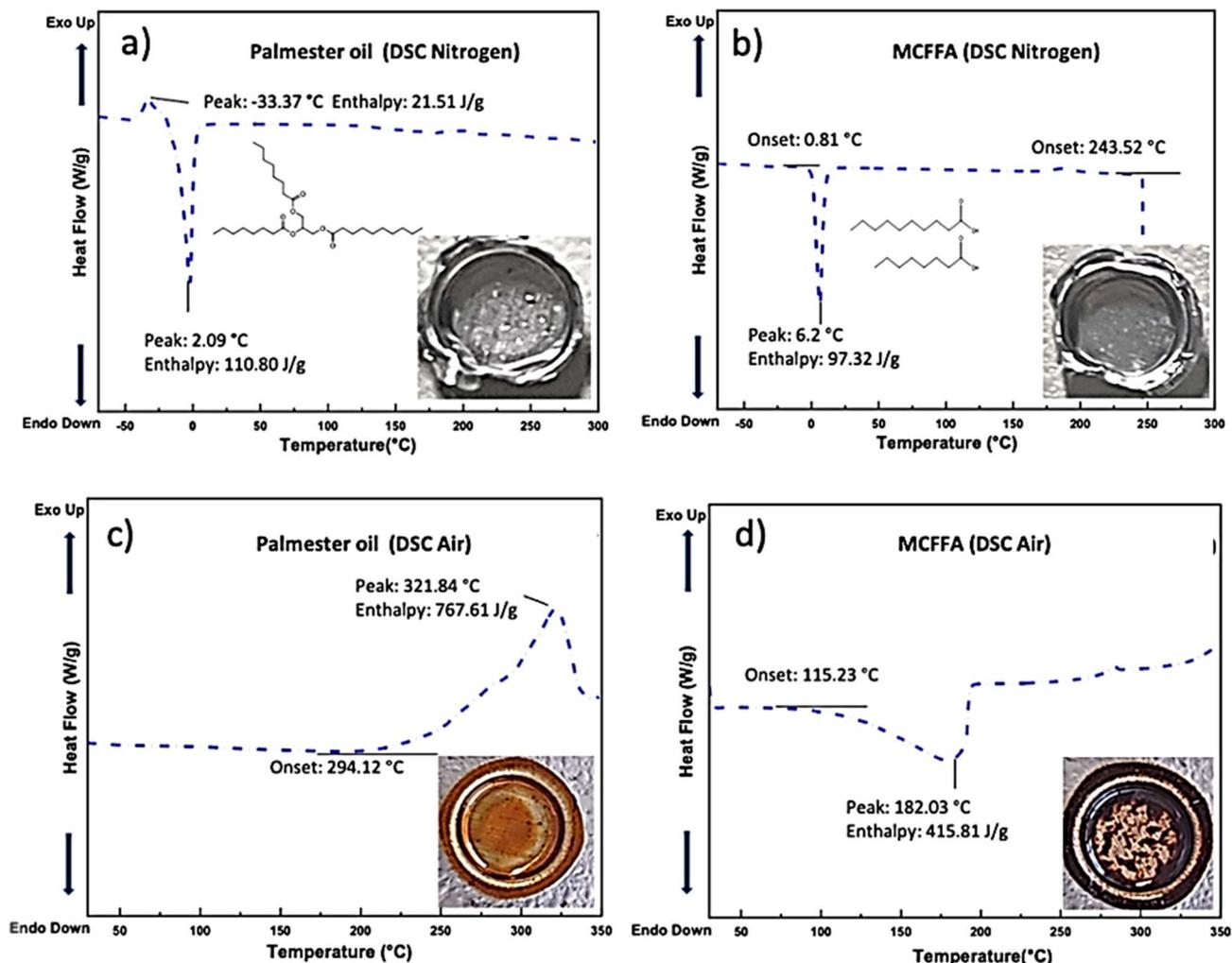
Fig. 7 DSC spectra of VFD-produced MCFFA and Palmester oil. The VFD was operated at 5000 rpm and 0.5 mL min^{-1} in continuous flow mode at 70 °C. (a and b) Samples were measured under the nitrogen atmosphere (DSC-250, temperature range was set from −70 °C to 300 °C). (c and d) Samples were measured under the air atmosphere (DSC-2000, the temperature range was 25 °C to 350 °C).

a Gram-negative bacterium, are commonly found in personal care products such as cosmetics, shampoos, lotions, and skincare products.[60] The cosmetics industry invests substantial resources into maintaining bacterial levels below regulatory standards. This study aims to assess whether the MCFFA produced from Palmester oil *via* VFD (60 : 40 mixture of caprylic and capric acids) offers enhanced antibacterial effectiveness against *S. aureus* and *E. coli*, exploring its potential in industry applications.

Ampicillin at 50 μg mL^{-1} was used as a positive control, showing significant antibacterial effects against both *S. aureus* and *E. coli*, while a 50% ethanol solution showed no zone of inhibition (ZOI), as shown in Table 2 and Fig. S3. There was no significant difference in the ZOI for ampicillin across all plates, confirming the reliability of the comparison of MCFFA antibacterial efficacy. Overall, *S. aureus* showed greater susceptibility to MCFFA. Notably, MCFFA exhibited superior performance in inhibiting *S. aureus*, producing ZOIs of 1.7 mm and 6.0 mm larger than those of commercial capric and caprylic

acids, respectively, at a concentration of 100 g L^{-1}. Furthermore, MCFFA displayed a ZOI of 24.33 mm at 50 g L^{-1}, 9 mm larger than caprylic acid, while capric acid showed no antibacterial activity at concentrations of 50 g L^{-1} and lower. In *E. coli*, MCFFA and caprylic acid produced comparable ZOIs at 100 g L^{-1} and at 50 g L^{-1}, but only MCFFA had a minor ZOI at 25 g L^{-1}. Capric acid once again showed no antibacterial activity at concentrations equal to and lower than 50 g L^{-1}, while no MCFFA had antibacterial effect at 12.5 g L^{-1}.

These data are consistent with the earlier report that caprylic acid is more effective against *E. coli*, fungi, and other microbes compared to capric, lauric, and longer-chain fatty acids.[60] Interestingly, MCFFA showed a ZOI at 25 g L^{-1}, while neither caprylic nor capric acid exhibited any inhibition. Our findings demonstrate that the mixture of caprylic and capric acids enhances antibacterial efficacy compared to its individual constituent fatty acids, particularly against *S. aureus*. Several mechanisms may contribute to this effect. The smaller size of caprylic acid may allow for rapid membrane penetration, while

Table 2 Antibacterial activity of VFD-produced MCFFA. The VFD was operated at 5000 rpm and 0.5 mL min^{-1} in continuous flow mode, at 70 °C. Commercial caprylic acid and capric acid serve as controls. A 50% ethanol solution is used as the negative control, while 50 μg per mL ampicillin is used as the positive control. When no ZOI was observed, the well diameter (7 mm) remained unchanged indicating no antibacterial effect, a ZOI of 0 is reported in these cases ($n = 3$)

		Positive control ampicillin (50 μg mL^{-1})	Negative control (50% ethanol)	MCFFA 100 g L^{-1}	MCFFA 50 g L^{-1}	MCFFA 25 g L^{-1}	MCFFA 12.5 g L^{-1}
S. aureus	MCFFA	25.0 ± 1.0	0.0	28.0 ± 1.7	24.3 ± 0.6	11.0 ± 1.0	0.0
	Capric acid (C10)	22.0 ± 1.0	0.0	26.3 ± 0.6	0.0	0.0	0.0
	Caprylic acid (C8)	25.7 ± 1.2	0.0	22.0 ± 1.0	15.3 ± 0.6	11.3 ± 0.6	0.0
E. coli	MCFFA	21.3 ± 1.5	0.0	20.3 ± 0.6	19.0 ± 1.0	9.0 ± 1.0	0.0
	Capric acid (C10)	22.3 ± 0.6	0.0	20.3 ± 0.6	0.0	0.0	0.0
	Caprylic acid (C8)	21.7 ± 0.6	0.0	22.0 ± 1.0	19.3 ± 0.6	0.0	0.0

capric acid provides more sustained disruption.[61] Their differences in solubility and lipophilicity enable them to target the bacterial membrane at varying rates and depths, creating a staggered attack that weakens the membrane further.[60,61] This disruption of the phospholipid membrane leads to leakage of cell contents and ultimately bacterial cell death. Gram-positive bacteria, like *S. aureus*, are especially vulnerable, as they lack the protective outer membrane present in Gram-negative bacteria.[60,62] We also examined the DPPH scavenging activity of MCFFA and found no significant difference between the samples (Fig. S4). This can be attributed to the stable structure of MCFFA, which lacks reactive groups to interact with DPPH radicals. Fatty acids with more C=C bonds may contribute more effectively to radical scavenging activity.[63]

4 Conclusion

This study demonstrates the production of high-purity MCFFA for antibacterial applications using VFD processing, offering enhanced efficiency and scalability for developing sustainable organic cosmetics. The VFD-confined mode was used for the optimisation study of optimal cost-efficiency. Additionally, continuous-mode VFD facilitated the scale-up of MCFFA production with a higher efficiency, purity, and yield compared to the traditional water bathing method. Specifically, VFD processing at 70 °C produced MCFFA with higher purity (96%) than water bath processing at 100 °C (70%). Analytical tests, including DSC, rheology, and viscosity measurements, revealed that MCFFA exhibited reduced viscosity and good thermal stability for cosmetic industry applications. Antibacterial testing further showed that MCFFA had greater efficacy against *S. aureus* than commercial caprylic and capric acids, highlighting its potential as a natural preservative for the organic cosmetics industry. Future research will investigate the biological applications of MCFFA, with an emphasis on its potential impacts on the skin barrier.

Author contributions

Xuejiao Cao: investigation, data curation, writing – original draft. Caterina Selva: data curation, formal analysis, visualisation. Jonathan Campbell: data curation, validation. Vincent Bulone: visualisation, supervision, data analysis. Xuan Luo:

data curation. Ajanth Praveen Mookkandi: validation; Youhong Tang: supervision, formal analysis; Colin Raston: visualisation, supervision, project administration, resources, funding acquisition.

Conflicts of interest

The authors declare no competing financial interest.

Data availability

The data supporting this article have been included as part of the supplementary information (SI). Supplementary information: (i) GC chromatograms and (ii) DSC thermograms of commercial caprylic and capric acids for comparative analysis; and (iii) antibacterial assay images and raw inhibition-zone measurements for *S. aureus* and *E. coli*, comparing VFD-produced MCFFA with commercial fatty acids at identical concentrations. See DOI: **https://doi.org/10.1039/d5su00610d**.

Acknowledgements

References

1 The Rise of Natural Cosmetic Ingredients in Response to Growing Demand for Clean and Sustainable Products, 2024 [cited 2025 18.04]; Available from: **https://www.databridgemarketresearch.com/whitepaper/the-rise-of-natural-cosmetic-ingredients-in-response**.

2 Sustainable strategy in cosmetic, part 2: Natural ingredients, 2024; Available from: https://erdyn.com/us/sustainable-strategy-in-cosmetic-part-2-natural-ingredients/.

3 Organic Certifications Explained! What Do All Those Letters Mean?, 2017 [cited 2025 11.05]; Available from: https://naturallysafe.com.au/naturally-safe-blog/organic-certifications-explained-what-do-all-those-letters-mean/.

4 About the COSMOS-standard, International Certification for Cosmetics, 2025, [cited 2025 11.15]; Available from: https://www.cosmos-standard.org/en/cosmos-standard/.

5 A. M. Martins and J. M. Marto, A sustainable life cycle for cosmetics: From design and development to post-use phase, *Sustainable Chem. Pharm.*, 2023, **35**, 101178.

6 COSMOS-standard Cosmetics Organic and Natural Standard, 2025 [cited 2025 11.05]; Available from: https://www.cosmos-standard.org/en/.

7 H. B. Jadhav and U. S. Annapure, Triglycerides of medium-chain fatty acids: a concise review, *J. Food Sci. Technol.*, 2023, **60**(8), 2143–2152.

8 A. R. Vaughn, *et al.*, Natural oils for skin-barrier repair: Ancient compounds now backed by modern science, *Am. J. Clin. Dermatol.*, 2018, **19**(1), 103–117.

9 M. Yang, M. Zhou and L. Song, A review of fatty acids influencing skin condition, *J. Cosmet. Dermatol.*, 2020, **19**(12), 3199–3204.

10 H. Hazarika, *et al.*, The fabrication and assessment of mosquito repellent cream for outdoor protection, *Sci. Rep.*, 2022, **12**(1), 2180.

11 M. Farooq, *et al.*, Efficacy Evaluation of Medium-Chain Fatty Acids as Skin and Spatial Repellents Against Aedes aegypti (Diptera:Culicidae) Mosquitoes, *J. Med. Entomol.*, 2023, **60**(2), 333–338.

12 Information., N. C. f. B., PubChem Compound, *Summary for CID 2969, Capric Acid*, 2024.

13 Information, N.C.f.B., PubChem Compound, *Summary for CID 379, Octanoic Acid*, 2024.

14 W. C. Lin, *et al.*, Octanoic acid promotes clearance of antibiotic-tolerant cells and eradicates biofilms of Staphylococcus aureus isolated from recurrent bovine mastitis, *Biofilm*, 2023, **6**, 100149.

15 T. M. Alharbi, *et al.*, Sub-micron moulding topological mass transport regimes in angled vortex fluidic flow, *Nanoscale Adv.*, 2021, **3**(11), 3064–3075.

16 M. Jellicoe, *et al.*, Vortex fluidic induced mass transfer across immiscible phases, *Chem. Sci.*, 2022, **13**(12), 3375–3385.

17 B. M. Alotaibi, *et al.*, Vortex Fluidic Mediated Synthesis of Enhanced Hydrogen Producing Magnetic Gold, *Small Sci.*, 2025, 2400449.

18 B. M. Alotaibi, *et al.*, Aqueous photo-induced high shear shape selective pristine silver nano/micro particles, *RSC Mechanochem.*, 2025, **2**(5), 653–661.

19 M. Jellicoe, *et al.*, Chiral Lemniscate Formation in Magnetic Field Controlled Topological Fluid Flows, *Small*, 2025, **21**(20), 2409807.

20 N. Joseph, *et al.*, Vortex fluidic regulated phospholipid equilibria involving liposomes down to sub-micelle size assemblies, *Nanoscale Adv.*, 2024, **6**(4), 1202–1212.

21 X. Luo, *et al.*, Printable Hydrogel Arrays for Portable and High-Throughput Shear-Mediated Assays, *ACS Appl. Mater. Interfaces*, 2023, 31114–31123.

22 X. Cao, *et al.*, Vortex fluidics mediated non-covalent physical entanglement of tannic acid and gelatin for entrapment of nutrients, *Food Funct.*, 2021, **12**(3), 1087–1096.

23 X. Luo, *et al.*, Sustainability-Driven Accelerated Shear-Mediated Immunoassay for Amyotrophic Lateral Sclerosis Detection, *ChemSusChem*, 2024, e202401008.

24 M. Jellicoe, *et al.*, High shear spheroidal topological fluid flow induced coating of polystyrene beads with C 60 spicules, *Chem. Commun.*, 2021, **57**(46), 5638–5641.

25 B. M. Alotaibi, *et al.*, Nanogold Foundry Involving High-Shear-Mediated Photocontact Electrification in Water, *Small Sci.*, 2024, 2300312.

26 Z. Gardner, *et al.*, High Shear Thin Film Synthesis of Partially Oxidized Gallium and Indium Composite 2D Sheets, *Small*, 2023, 2300577.

27 X. Cao, *et al.*, Stability and Cleansing Function Enhancement of Organic Shampoo by a Vortex Fluidic Device, *ACS Sustain. Chem. Eng.*, 2024, **12**(14), 5533–5543.

28 E. K. Sitepu, *et al.*, Vortex fluidic mediated direct transesterification of wet microalgae biomass to biodiesel, *Bioresour. Technol.*, 2018, **266**, 488–497.

29 J. Britton, *et al.*, Vortex fluidic chemical transformations, *Chem.–Eur. J.*, 2017, **23**(54), 13270–13278.

30 J. Britton, J. M. Chalker and C. L. Raston, Rapid vortex fluidics: continuous flow synthesis of amides and local anesthetic lidocaine, *Chem.–Eur. J.*, 2015, **21**(30), 10660–10665.

31 S. He, *et al.*, Upsized Vortex Fluidic Device Enhancement of Mechanical Properties and the Microstructure of Biomass-Based Biodegradable Films, *ACS Sustainable Chem. Eng.*, 2021, **9**(43), 14588–14595.

32 A. Jaber, *et al.*, Interfacial viscoelastic moduli in a weak gel, *J. Colloid Interface Sci.*, 2022, **622**, 126–134.

33 J. Britton, S. B. Dalziel and C. L. Raston, Continuous flow Fischer esterifications harnessing vibrational-coupled thin film fluidics, *RSC Adv.*, 2015, **5**(3), 1655–1660.

34 Y.-Y. Lee, *et al.*, Medium chain triglyceride and medium-and long chain triglyceride: metabolism, production, health impacts and its applications–a review, *Crit. Rev. Food Sci. Nutr.*, 2022, **62**(15), 4169–4185.

35 M. Hasanpour, *et al.*, 1H NMR-based metabolomics study of the lipid profile of omega-3 fatty acid supplements and some vegetable oils, *J. Pharm. Biomed. Anal.*, 2024, **238**, 115848.

36 E. Menalla, *et al.*, Hydrothermal hydrolysis of triglycerides: Tunable and intensified production of diglycerides, monoglycerides, and fatty acids, *Chem. Eng. J.*, 2024, **493**, 152391.

37 B. Chen, *et al.*, A Novel Data Fusion Strategy of GC-MS and 1H NMR Spectra for the Identification of Different Vintages of Maotai-flavor Baijiu, *J. Agric. Food Chem.*, 2024, **72**(26), 14865–14873.

38 E. K. Sitepu, *et al.*, Critical evaluation of process parameters for direct biodiesel production from diverse feedstock, *Renewable Sustainable Energy Rev.*, 2020, **123**, 109762.

39 X. Luo, et al., Sustainability-Driven Accelerated Shear-Mediated Immunoassay for Amyotrophic Lateral Sclerosis Detection, ChemSusChem, 2024, e202401008.

40 K. M. Abed, et al., Superiority of liquid membrane-based purification techniques in biodiesel downstream processing, Renewable Sustainable Energy Rev., 2025, 207, 114911.

41 X. Cao, et al., Vortex fluidic mediated generation of fatty acid ethyl esters from vegetable oils for applications in cosmetic emulsions, J. Clean. Prod., 2025, 494, 145006.

42 N. L. Rozali, et al., Fourier transform infrared (FTIR) spectroscopy approach combined with discriminant analysis and prediction model for crude palm oil authentication of different geographical and temporal origins, Food Control, 2023, 146, 109509.

43 I. Zojaji, A. Esfandiarian and J. Taheri-Shakib, Toward molecular characterization of asphaltene from different origins under different conditions by means of FT-IR spectroscopy, Adv. Colloid Interface Sci., 2021, 289, 102314.

44 R. H. Ellerbrock and H. H. Gerke, FTIR spectral band shifts explained by OM–cation interactions, J. Plant Nutr. Soil Sci., 2021, 184(3), 388–397.

45 N. García, et al., Sensory properties analysis of a calcipotriol and betamethasone dipropionate cream vehicle formulated with an innovative PAD Technology for the treatment of plaque psoriasis on the skin and scalp, Drugs Context, 2023, 12, 2023.

46 T. Tadros, Cosmetics, in Encyclopedia of Colloid and Interface Science, ed. T. Tadros, Springer Berlin Heidelberg, Berlin, Heidelberg, 2013, pp. 148–207.

47 C. Yacine, et al., Rheological behavior and microstructural properties of crude oil and emulsions (water/oil-oil/water), Pet. Sci. Technol., 2024, 42(9), 1047–1063.

48 A. Bisht, et al., Does harvesting age matter? Changes in structure and rheology of a shear-thickening polysaccharide from Cyathea medullaris as a function of age, Carbohydr. Polym., 2024, 329, 121757.

49 M. Shahbazi, H. Jäger and R. Ettelaie, Application of Pickering emulsions in 3D printing of personalized nutrition. Part I: Development of reduced-fat printable casein-based ink, Colloids Surf., A, 2021, 622, 126641.

50 F. C. César and P. M. Maia Campos, Influence of vegetable oils in the rheology, texture profile and sensory properties of cosmetic formulations based on organogel, Int. J. Cosmet. Sci., 2020, 42(5), 494–500.

51 S. Calligaris, et al., Phase Transition of Sunflower Oil as Affected by the Oxidation Level, J. Am. Oil Chem. Soc., 2008, 85, 591–598.

52 P. J. Sinko, Chapter Objectives, Martin's Physical Pharmacy and Pharmaceutical Sciences, 2023.

53 Y. Liu, et al., Bamboo-based cellulose nanofibers as reinforcement for polyurethane imitation wood, Ind. Crops Prod., 2024, 210, 118177.

54 J. T. Cullen, T. Kärkelä and U. Tapper, Signatures that differentiate thermal degradation and heterogeneous combustion of tobacco products and their respective emissions, J. Anal. Appl. Pyrolysis, 2024, 179, 106478.

55 M. Saldaña and S. Martínez-Monteagudo, Oxidative stability of fats and oils measured by differential scanning calorimetry for food and industrial applications, Applications of Calorimetry in a Wide Context—Differential Scanning Calorimetry, Isothermal Titration Calorimetry and Microcalorimetry, 2013, p. 449.

56 V. Chiaia, et al., Study of oxidation products in aged olive oils by GC and HPLC techniques coupled to mass spectrometry to discriminate olive oil lipid substances in archaeological artifacts from ancient Taormina (Italy), J. Chromatogr. A, 2024, 1731, 465154.

57 A. Alinezhad, et al., Mechanistic Investigations of Thermal Decomposition of Perfluoroalkyl Ether Carboxylic Acids and Short-Chain Perfluoroalkyl Carboxylic Acids, Environ. Sci. Technol., 2023, 57(23), 8796–8807.

58 H. Arellano, et al., Saturated long chain fatty acids as possible natural alternative antibacterial agents: Opportunities and challenges, Adv. Colloid Interface Sci., 2023, 318, 102952.

59 J. A. Jackman, R. D. Boyd and C. C. Elrod, Medium-chain fatty acids and monoglycerides as feed additives for pig production: towards gut health improvement and feed pathogen mitigation, J. Anim. Sci. Biotechnol., 2020, 11(1), 44.

60 N. Nusrat, et al., Assessment of potential pathogenic bacterial load and multidrug resistance in locally manufactured cosmetics commonly used in Dhaka metropolis, Sci. Rep., 2023, 13(1), 7787.

61 G. Casillas-Vargas, et al., Antibacterial fatty acids: An update of possible mechanisms of action and implications in the development of the next-generation of antibacterial agents, Prog. Lipid Res., 2021, 82, 101093.

62 T. J. Foster and J. A. Geoghegan, Chapter 34 - Staphylococcus aureus, in Molecular Medical Microbiology, ed. Y.-W. Tang, et al., Academic Press, 3rd edn, 2024, pp. 655–679.

63 T. Phengnuam, et al., DPPH radical scavenging activity of a mixture of fatty acids and peptide-containing compounds in a protein hydrolysate of Jatropha curcas seed cake, J. Agric. Food Chem., 2013, 61(48), 11808–11816.